Science
AAAS

Supplementary Materials for

A single mutation in bovine influenza H5N1 hemagglutinin switches specificity to human receptors

Ting-Hui Lin *et al*.

Corresponding authors: James C. Paulson, jpaulson@scripps.edu; Ian A. Wilson, wilson@scripps.edu

Science **386**, 1128 (2024)
DOI: 10.1126/science.adt0180

The PDF file includes:

Materials and Methods
Figs. S1 to S8
Tables S1 and S2
References

Other Supplementary Material for this manuscript includes the following:

MDAR Reproducibility Checklist

Materials and Methods

Expression and purification of soluble recombinant H5N1 HA protein

The sequence for influenza A/Texas/37/2024 H5N1 HA was downloaded from Global Initiative on Sharing All Influenza Data (GISAID) (*74*). The ectodomain of HA sequence was subcloned into pFastbac-1 expression vector with N-terminal gp67 secreted signal peptide and a C-terminal trimerization domain followed by a thrombin site and 6x His-tag. The recombinant baculoviruses with HA gene were generated using a Bac-to-Bac baculovirus expression system in Sf9 cells (Thermo Fisher Scientific) as described previously (*75*). The recombinant soluble HA proteins were expressed in High Five cells (Thermo Fisher Scientific) with an MOI of 5-10 for each recombinant virus. After 72 hours, the soluble HA proteins were harvested from supernatant and then further clarified by centrifugation. The soluble HA proteins in clarified supernatant were purified by metal-affinity chromatography using Ni-nitrilotriacetic acid (Ni-NTA) resin (Qiagen) and buffer-exchanged into Tris-buffered saline (TBS, pH 8.0). The purified HA proteins were digested with trypsin in a final ratio of 1:1000 (wt/wt) and then further purified by size exclusion chromatography (SEC) using HiLoad 16/90 Superdex 200 column (GE Healthcare). Proteins produced in insect cells contain paucimannose N-glycans and lack more complex terminal glycans, such as sialylated N-glycans. In contrast, proteins expressed in mammalian cells are more complex, featuring different branching and terminal modifications. Glycans, especially those located near the receptor-binding site, can create steric hindrance for protein binding to their receptors. Whole virus expressed from eggs and MDCK cells exhibit similar binding patterns to HA expressed from insect cells (*44*), although one report shows that soluble HAs expressed with sialylated glycans in mammalian cells can exhibit different fine specificities to sialosides on a glycan microarray compared to HA expressed in insect cells, but these differences were abrogated when the HA glycans were desialylated as would naturally occur on the HA of virions due to the influenza neuraminidase (*76*). We would also expect here that the receptor binding specificity would be largely unaffected by expression of the Texas H5 HA in different platforms as there are no N-glycans proximal to the receptor binding site as there was in the mammalian study with H2 and H7 HAs (*76*). The purified HAs were used for the structure and binding studies.

Crystallization, data collection, and structure determination for HA and HA-receptor analogs complex.

The purified soluble HA proteins were concentrated to 10 mg/ml for crystallization trials. The initial crystallization condition for apo-HA (unliganded HA) was obtained from crystal screening on our automated Rigaku CrystalMation system at The Scripps Research Institute using JCSG Core Suite (QIAGEN) as precipitant. The crystallization screening was based on the sitting drop vapor diffusion method by mixing 0.1 µl of protein with 0.1 µl of the reservoir solution. To facilitate the crystallization of WT A/Texas/37/2024 H5N1 HA, we introduced a mutation (D240N) based on an H5 structure that we determined previously (*77*). This mutation is far from the receptor binding site. The optimized crystallization conditions were: 0.1 M Hepes, pH 6.7, 15% PEG6000 for apo-Texas HA; and 0.1M Hepes pH 6.9, 18% PEG6000 for Leu^{226}-Texas HA. Crystals were harvested after one week and then soaked in a reservoir solution with 10% (v/v) ethylene glycol as cryoprotectant. For HA-receptor analogs complexes, we used LSTa (Neu5Acα2-3Galβ1-3GlcNAcβ1-3Galβ1-4Glc), and LSTc (Neu5Acα2-6Galβ1-3GlcNAcβ1-3Galβ1-4Glc). Apo-crystals were harvested and then soaked with ligands at a final concentration of 5 mM in the reservoir solution for 5-20 minutes. The crystals were then stored in liquid nitrogen until data collection. Diffraction data for Apo-HA and HA-ligand complexes were collected at

synchrotron radiation beamlines specified on the crystal data collection and statistics table S1. HKL2000 was used for data processing (*78*). Initial phases for apo-HA and HA-ligand complexes were solved by molecular replacement using Phaser with H5 HA (PDB: 5E30) as a model (*79*). Manual refinement was carried out in Coot and PHENIX (*80, 81*). For the LSTc complex, only one monomer of the HA trimer had interpretable density for all five sugar moieties of LSTc, whereas another HA monomer had well-resolved density for three to four monosaccharides, and the third monomer of the HA trimers does not have ligand built because of poor ligand density. Final refinement statistics for each crystal structure are summarized in table S1.

Preparation of biotinylated sialosides

A library of biotinylated sialosides composed of linear and N-linked glycans carrying one to three LacNAc repeats were synthesized essentially as previously described (*82*). As a final enzymatic step, linear and N-linked glycans were sialylated using either recombinant human ST6Gal-I to add sialic acid in an α2-6 linkage, or rat ST3Gal-III to add sialic acid in an α2-3 linkage. Biotinylation of the NH_2-terminated linker of the sialosides was achieved with NHS-LCLC-biotin (Thermo Scientific, cat no. 21343) and DIPEA (Sigma-Aldrich, cat no. 496219). All biotinylated glycans were confirmed by high-resolution mass spectrometry (HRMS) as follows: **3SLN$_1$-L**, ESI TOF-HRMS m/z calculated for $C_{49}H_{84}N_7O_{23}S$, $[M + H]^+$: 1170.5334, found 1170.5379; **3SLN$_2$-L**, ESI TOF-HRMS m/z calculated for $C_{63}H_{108}N_8O_{33}S$, $[M + 2H]^{2+}$: 768.3364, found 768.3373; **3SLN$_3$-L**, ESI TOF-HRMS m/z calculated for $C_{77}H_{131}N_9O_{43}S$, $[M + 2H]^{2+}$: 950.9025, found 950.9019; **3SLN$_1$-N**, ESI TOF-HRMS m/z calculated for $C_{112}H_{181}N_{13}O_{69}S$, $[M - 2H]^{2-}$: 1422.5409, found 1422.5355; **3SLN$_2$-N**, ESI TOF-HRMS m/z calculated for $C_{140}H_{226}N_{15}O_{89}S$, $[M - 3H]^{3-}$: 1191.4463, found 1191.4417; **3SLN$_3$-N**, ESI TOF-HRMS m/z calculated for $C_{168}H_{273}N_{17}O_{109}S$, $[M - 3H]^{3-}$: 1435.2037, found 1435.1959; **6SLN$_1$-L**, ESI TOF-HRMS m/z calculated for $C_{49}H_{84}N_7O_{23}S$, $[M + H]^+$: 1170.5334, found 1170.5367; **6SLN$_2$-L**, ESI TOF-HRMS m/z calculated for $C_{63}H_{108}N_8O_{33}S$, $[M + 2H]^{2+}$: 768.3364, found 768.3401; **6SLN$_3$-L**, ESI TOF-HRMS m/z calculated for $C_{77}H_{131}N_9O_{43}S$, $[M + 2H]^{2+}$: 950.9025, found 950.9023; **6SLN$_1$-N**, ESI TOF-HRMS m/z calculated for $C_{110}H_{182}N_{12}O_{68}S$, $[M + 2H]^{2+}$: 1396.0448, found 1396.0477; **6SLN$_2$-N**, ESI TOF-HRMS m/z calculated for $C_{138}H_{229}N_{14}O_{88}S$, $[M + 3H]^{3+}$: 1174.4538, found 1174.4567; **6SLN$_3$-N**, ESI TOF-HRMS m/z calculated for $C_{166}H_{276}N_{16}O_{108}S$, $[M + 3H]^{3+}$: 1418.2117, found 1418.2285.

ELISA

The recombinant purified HAs used in ELISA were concentrated to 3-5 mg/ml. Briefly, extended linear and biantennary α2-3 and α2-6 sialosides with biotin tag were incubated in streptavidin-coated high binding capacity 384-well plates (Pierce) in PBS, pH 7.4 at 4ºC for 12 hours. Excess glycans were removed by washing with PBS containing 0.05% Tween-20 (PBST). The plates were then blocked with 1% bovine serum albumin (BSA) in PBS (BSA/PBS) buffer containing 0.6 μM desthiobiotin for 2 hours. After 2 hours, the plates were washed with PBST three times before further assay. The HA proteins with His-tag were incubated with anti-His mouse IgG2a primary antibody (BioLegend, cat no. 362616) and HRP-conjugated goat anti-mouse IgG (H + L) secondary antibody (Invitrogen, cat no. G21040) in a 4:2:1 ratio (w/w/w) in BSA/PBS buffer and incubated on ice for 30 min. The HA-antibody complexes were then 3-fold serially diluted and transferred to glycan-coated plates and incubated at room temperature for 2 hours. The plates were then washed and 3,3′,5,5′ tetramethylbenzidine (TMB, Sigma-Aldrich, cat no. T0440) peroxidase substrate added to each well for 15 min at room temperature. The reaction was quenched by adding

2 M sulfuric acid and binding detected at 450 nm absorbance using a BioTek Synergy H1 microplate reader (Agilent). Each HA-glycan analysis in ELISA was performed in duplicate. *Maackia amurensis* agglutinin (MAA) and *Sambucus nigra* agglutinin (SNA) were used as experimental positive controls for binding to α2-3 and α2-6 sialosides, respectively.

Glycan array

Glycan microarray was generated and used in influenza HA receptor specificity evaluation as previously described (*82, 83*). The His-tagged HAs were incubated with anti-His mouse IgG2a primary antibody (BioLegend, cat no. 362616) and HRP-conjugated goat anti-mouse IgG (H + L) secondary antibody (Invitrogen, A001) in TBST in a 4:2:1 ratio on ice for 30 min. The HA-antibody mixtures were transferred to the microarray with six replicates of each glycan and incubated at room temperature for 60 min. After 60 min, the slides were washed with PBST twice, then water, and dried before scanning by an Innoscan 1100AL microarray scanner (Innopsys).

Surface plasmon resonance

SPR measurements were conducted on a Biacore S200 at room temperature. TBST (TBS with 0.005% Tween-20) buffer was used as running buffer and to reconstitute all protein and glycan molecules. The linear α2-6 tri-LacNAc ($6SLN_3$-L, human receptor analogs) and α2-3 tri-LacNAc ($3SLN_3$-L, avian receptor analogs) with biotin tag were immobilized on the chips (Cytiva SA S series chips). The immobilized level was targeted to 500 RU (response unit). A blank flow cell was treated in parallel without glycan injection. After immobilization, multicycle kinetic measurements were conducted on each recombinant hemagglutinin analyte. 5000 nM, 2500 nM, 1250 nM, 625 nM, 312.5 nM, 156.3 nM, 78.1 nM, 39.1 nM, 19.5 nM, 9.8 nM, 4.9 nM and 0 nM analyte were injected at 30 μL/min for 120 s and followed by 240 s dissociation. After each cycle, 2 steps of 30 s regeneration with pH 2.7 glycine buffer were used to achieve a flat baseline signal. Final SPR sensorgrams were collected by reference channel subtraction and zero concentration subtraction. Static state affinity was calculated by Biacore evaluation software. The K_D values for WT-Texas HA against $3SLN_3$-L and $6SLN_3$-L were calculated by Biacore S200 evaluation software static affinity model.

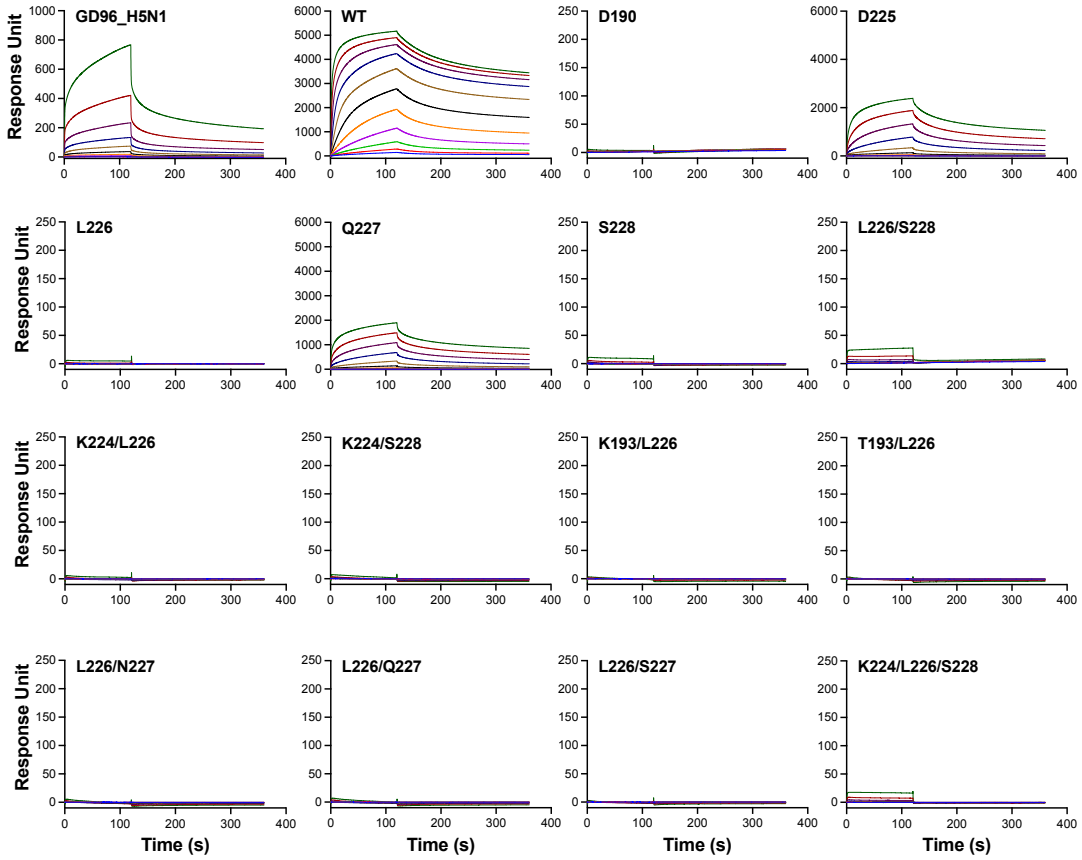

Fig. S1. Receptor binding of bovine Texas H5 HA mutants to α2-3 sialylated glycans using SPR. Biacore diagrams representing the binding of each mutant to α2-3 tri-LacNAc ($3SLN_3$-L). The y-axis shows the response. The response curves for different analyte concentrations are shown in different colors. Binding affinities were measured for wild-type and each HA mutant at 2-fold dilutions starting from 5 μM. A/goose/Guangdong/1/1996 (GD96_H5N1) HA was used as an avian control for binding to α2-3 sialosides. This figure is related to Figs. 1 and 2, figs. S2 and S3.

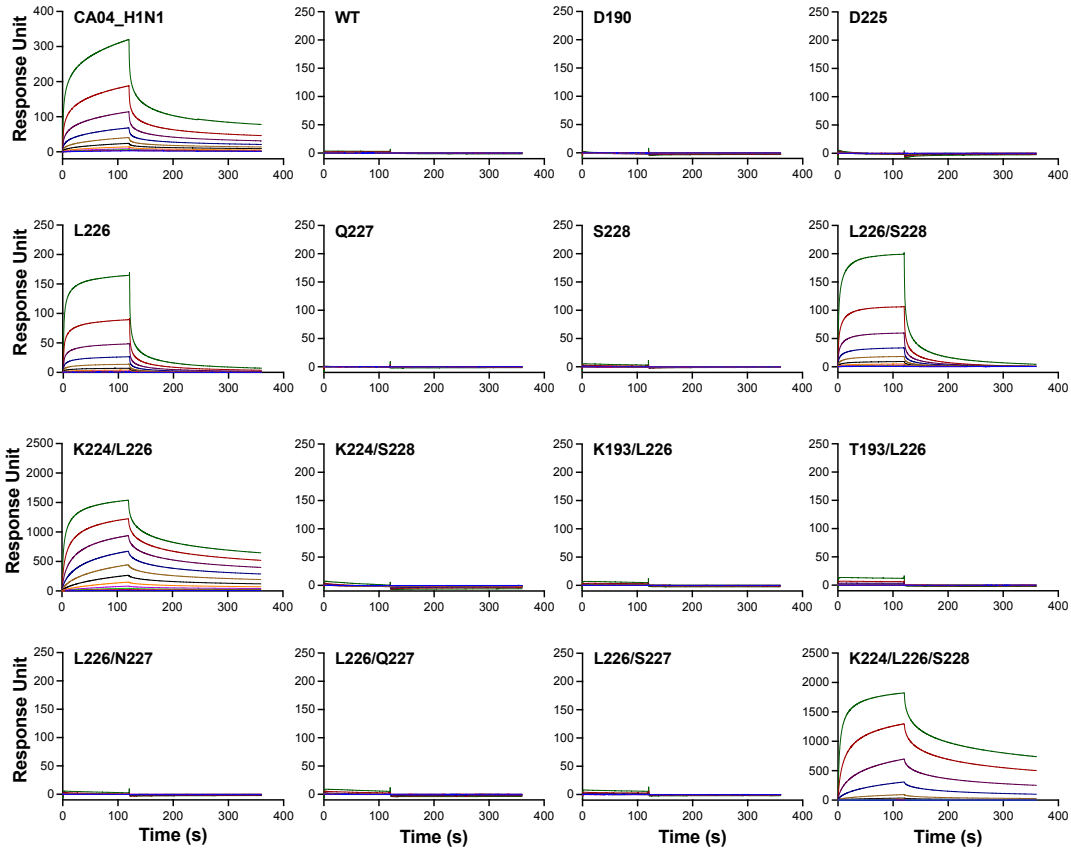

Fig. S2. Receptor binding of bovine Texas H5 HA mutants to α2-6 sialylated glycans by SPR. Biacore diagrams of the binding of each mutant to α2-6 tri-LacNAc (6SLN$_3$-L). The y-axis shows the response. The response curves for different analyte concentrations are represented in different colors. Binding affinities were measured for wild-type and each HA mutant at 2-fold dilutions starting from 5 μM. A/California/04/09 (CA04) H1 HA was used as a positive control. This figure is related to Figs. 1 and 2, figs. S1 and S3.

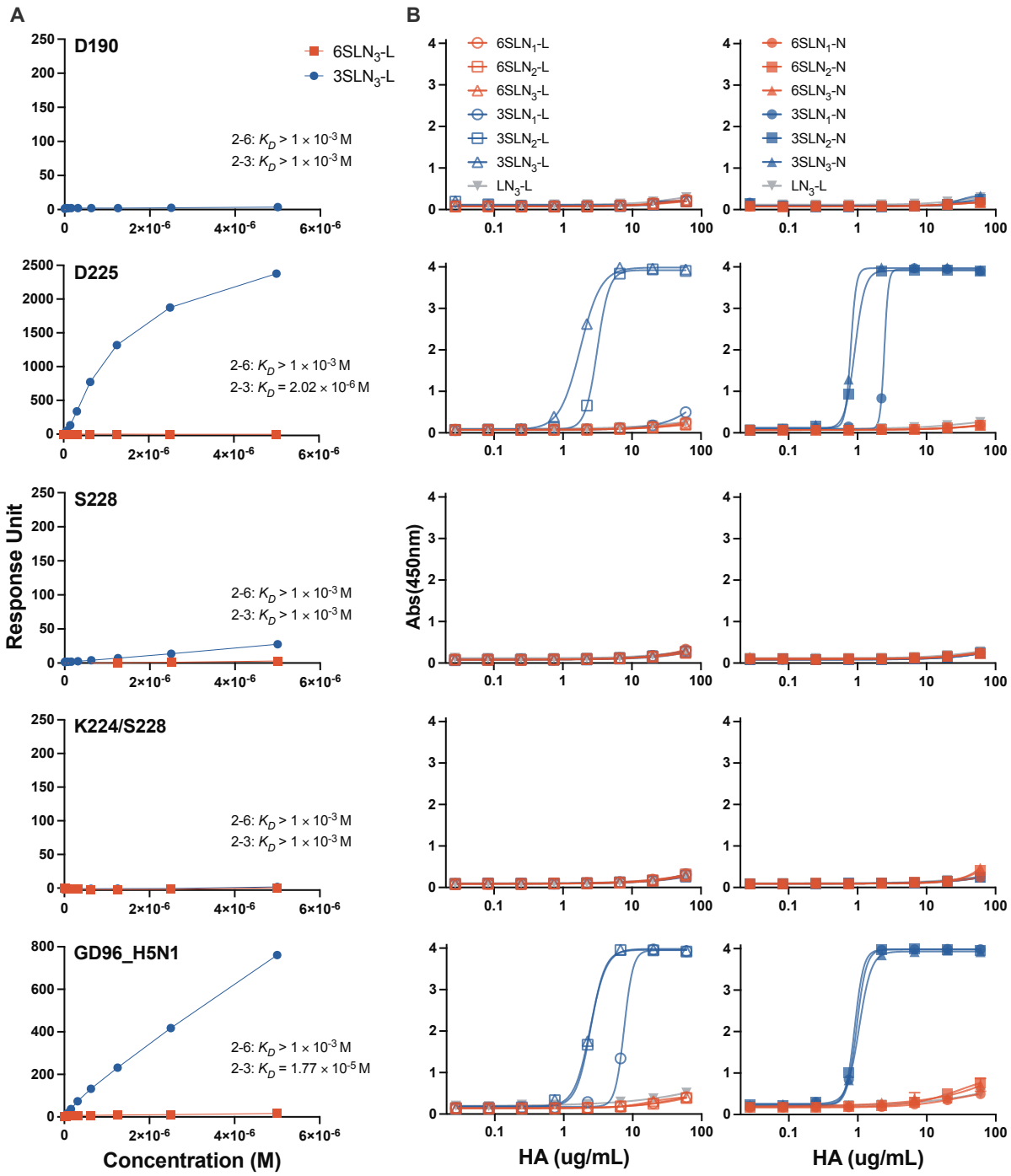

Fig. S3. Receptor binding specificity of bovine Texas H5 HA mutants by SPR and ELISA. Binding of Asp^{190}, Asp^{225}, Ser^{228}, and Lys^{224}/Ser^{228} mutants to α2-3 and α2-6 sialosides were measured by SPR (**A**) and ELISA (**B**). The estimated K_D for each mutant was calculated by Biacore S200 evaluation software static affinity model. The response curves for the SPR assays are shown in figs. S1 and S2. The extended linear (left panel, open shapes) and biantennary (right panel, solid shapes) α2-3 (blue) and α2-6 sialosides (red) were used in the ELISA. Glycans for α2-3 and α2-6 sialosides are represented in Fig. 1. The H5 HA from A/goose/Guangdong/1/1996 (GD96_H5N1) was used as H5 avian control for binding to α2-3 sialosides.

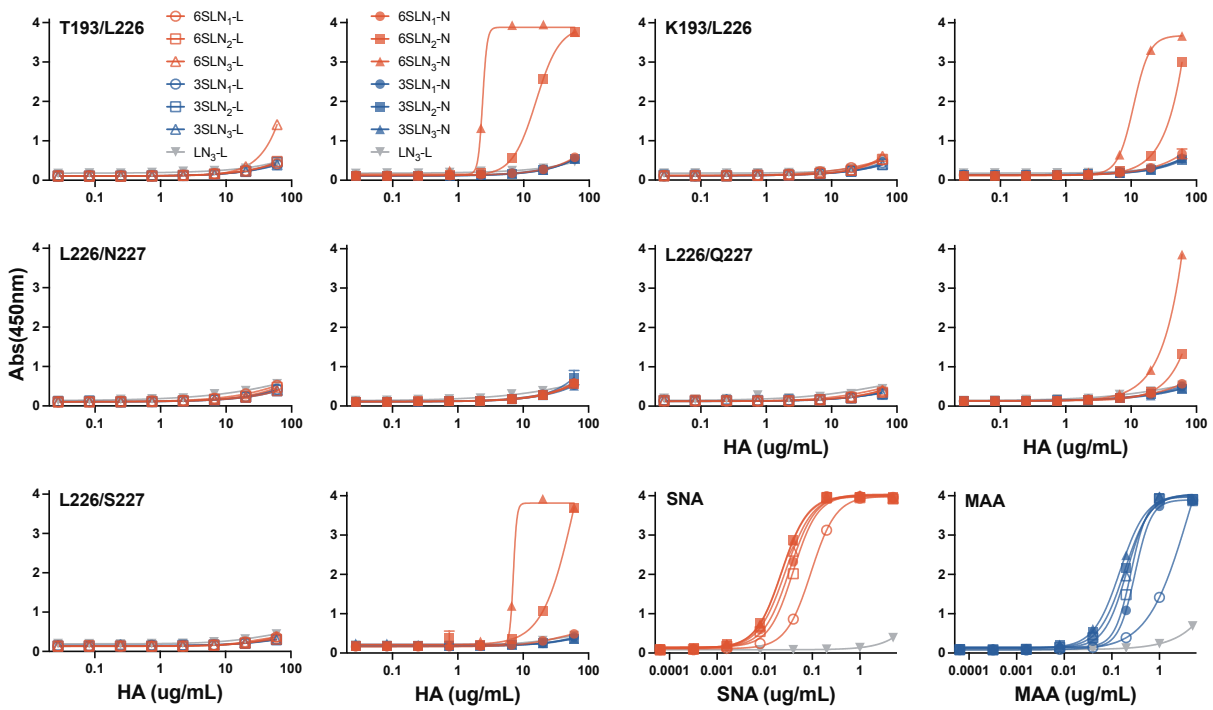

Fig. S4. Receptor binding specificity of bovine Texas H5 HA Leu^{226} mutant with other mutations measured by ELISA. Glycan binding of the Leu^{226} mutant with Thr^{193}, Lys^{193}, Asn^{227}, Gln^{227}, and Ser^{227} mutations was measured by ELISA with the extended linear (open shapes) and biantennary (solid shapes) α2-3 (blue) and α2-6 (red) sialosides. *Maackia amurensis* agglutinin (MAA) and *Sambucus nigra* agglutinin (SNA) were used as experimental controls for binding to α2-3 and α2-6 sialosides throughout the ELISA experiments in this study. LN_3-L with no sialic acid was used as a control.

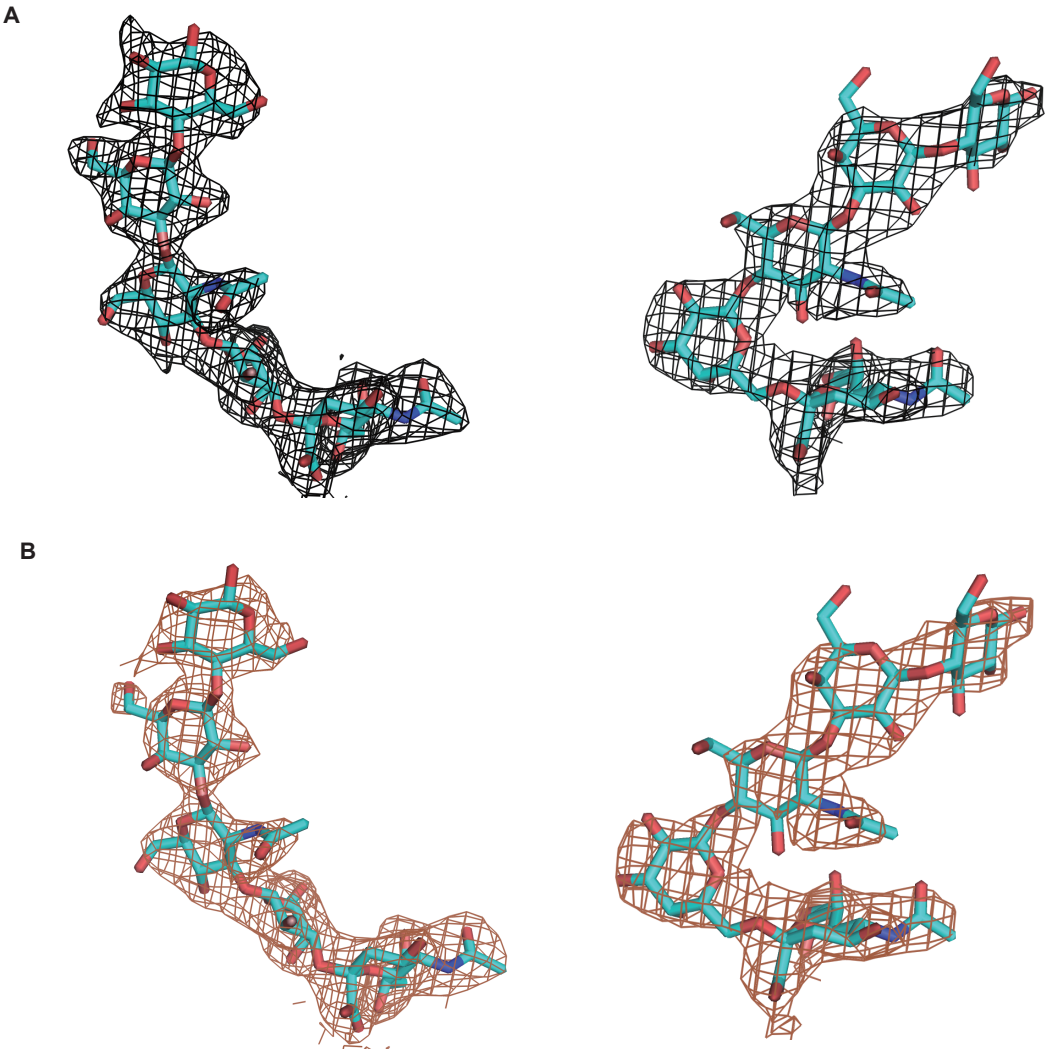

Fig. S5. Electron density maps of avian and human receptors in the crystal structures of bovine Texas H5 HA-ligand complexes. 2Fo-Fc (**A**) and 2Fo-Fc unbiased omit (**B**) electron density maps for each ligand are contoured at a 1 σ level and represented in black and brown mesh with the refined structures superimposed, respectively. LSTa (NeuAcα2-3Galβ1-3GlcNAcβ1-3Galβ1-4Glc) from WT Texas HA - LSTa complex (left). LSTc (NeuAcα2-6Galβ1-4GlcNAcβ1-3Galβ1-4Glc) from Texas HA Leu^{226} mutant - LSTc complex (right).

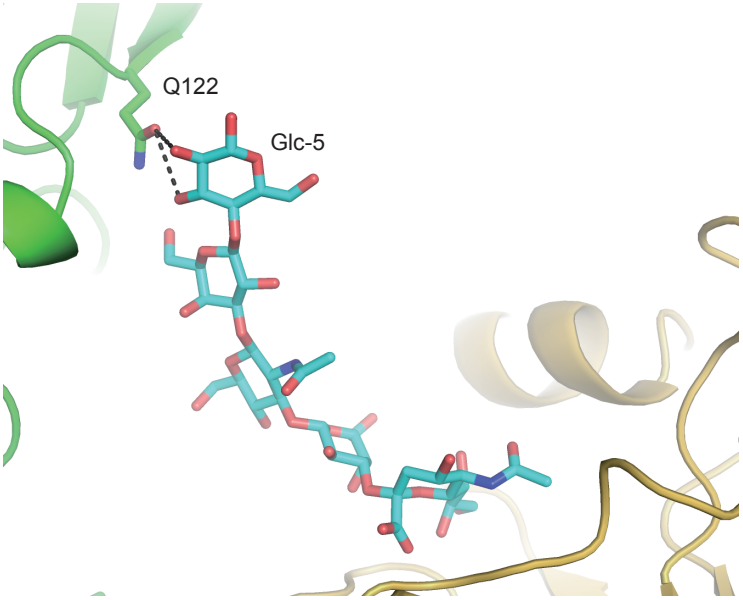

Fig. S6. Avian receptor analog LSTa contacts a symmetry-related HA in the crystal structure with bovine Texas H5 HA. The receptor binding site (RBS) of WT Texas H5 HA is depicted in a gold backbone cartoon. LSTa is shown with cyan carbons. An adjacent HA in a symmetry-related molecule is represented as a green backbone cartoon. Hydrogen bonds between LSTa Glc-5 and a symmetry-related HA are indicated in black dashes.

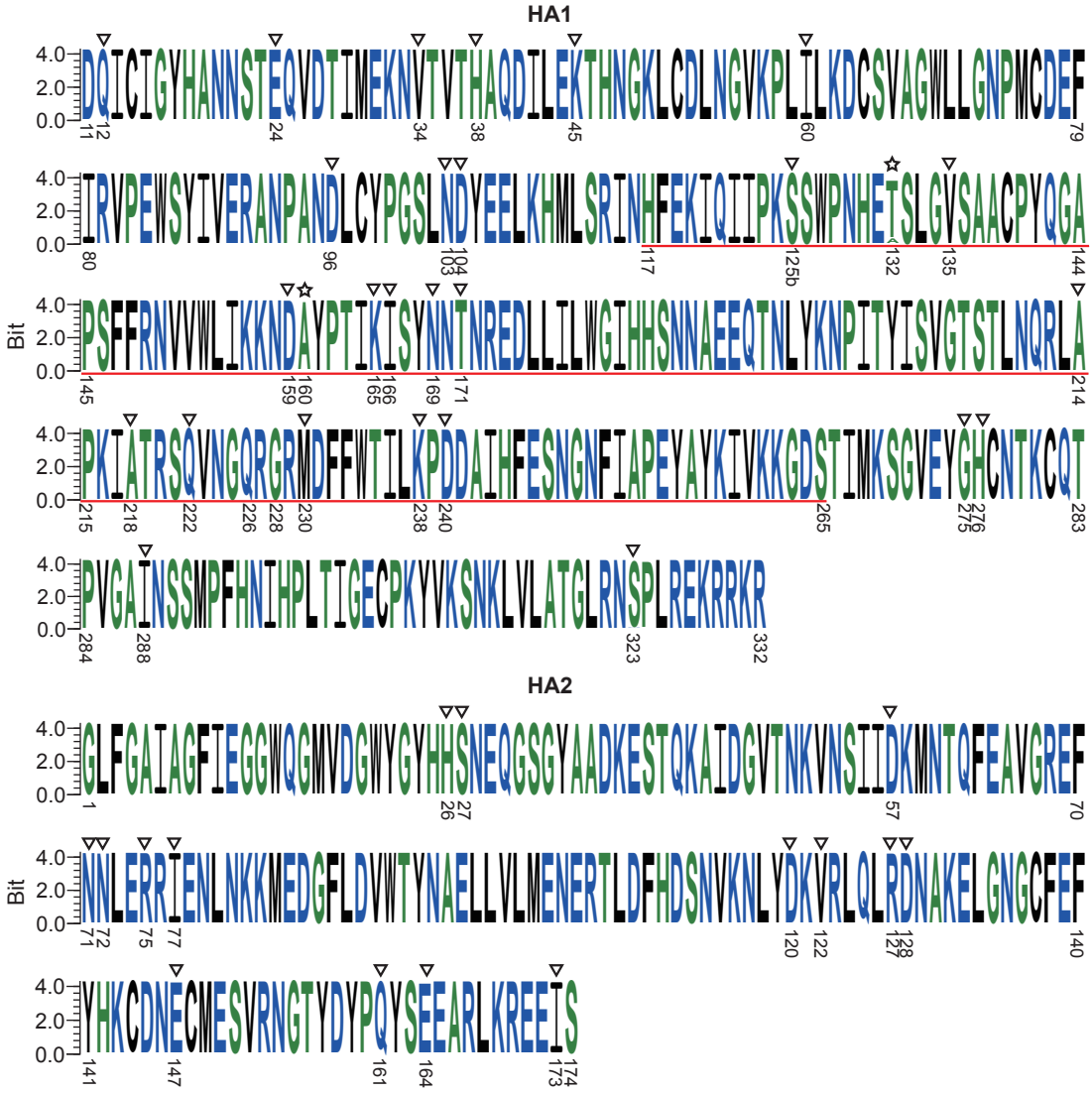

Fig. S7. Frequency of amino acids at HA residues in bovine influenza viruses. Weblogo plot were generated by using weblogo3. A total of 900 HA sequences collected and isolated from bovine influenza viruses from January 1, 2024 to October 1, 2024 in GISAID were analyzed and represented as HA1 and HA2. The red underline indicates residues that comprise the receptor binding subdomain. A triangle (▽) indicate mutations that are observed in fewer than 3 strains, while a star (☆) denotes mutations detected in more than 10 strains (for a total of 83 and 13 mutations observed at HA positions 132 and 160, respectively). The Ala to Thr mutation at residue 160 leads to a glycosylation site at Asn[158]. H3 HA numbering is used. The mutations are so rare compared to the total sequences analyzed that no mutations show up on the logo plot.

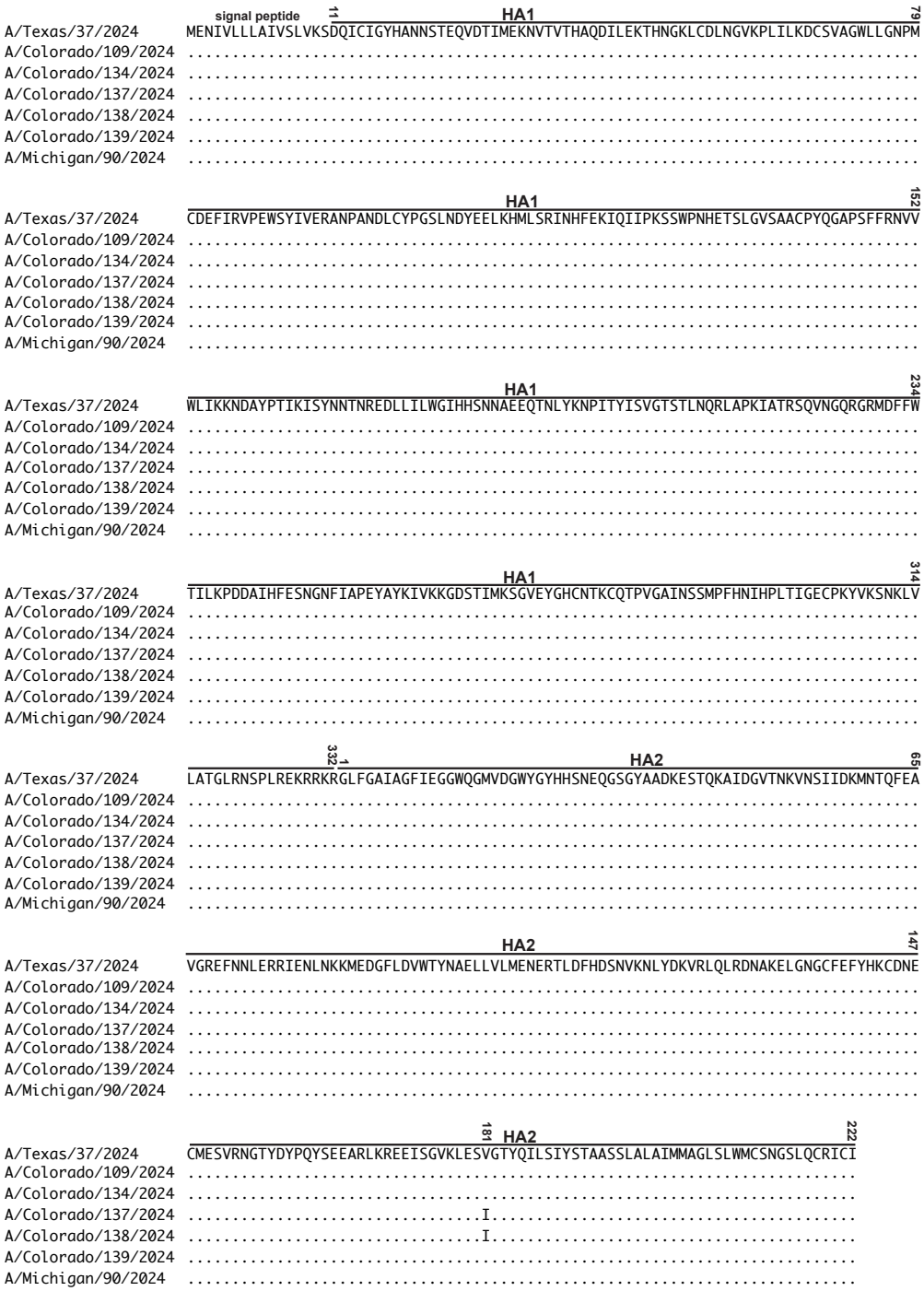

Fig. S8. Sequence alignment of HA from human infections with 2.3.4.4b H5N1 influenza viruses. A total 7 HA sequences from human infection with bovine and bird H5N1 influenza viruses deposited in GISAID this year were analyzed. Sequence variation after alignment with A/Texas/37/2024 is shown with a letter if a residue differs from A/Texas/37/2024 and with a dot (.) for conserved residues. H3 HA numbering is used.

Table S1. X-ray data collection and refinement statistics

Data collection	Apo-Texas H5	Texas H5/LSTa	L226-Texas H5/LSTc
Beamline	SSRL12-1	SSRL12-1	NSLSII 17-ID-2
Wavelength (Å)	0.9795	0.9795	0.9793
Space group	$P2_1$	$P2_1$	C2
Unit cell parameters			
a, b, c (Å)	130.4 72.1 206.9	103.5 74.8 131.1	254.4 214.5 136.0
α, β, γ (°)	90 91.7 90	96, 96.2, 90	90, 115.1, 90
Resolution (Å) [a]	50.0-2.70 (2.75-2.70)	50.0-2.32 (2.36-2.32)	50.0-2.70 (2.75-2.70)
Unique reflections [a]	103,266 (9020)	85,341 (8523)	177,926 (17,078)
Redundancy [a]	3.9 (3.8)	6.7 (6.3)	6.8 (6.5)
Completeness (%) [a]	98 (98)	99 (99)	100 (100)
$<I/\sigma_I>$ [a]	8.5 (0.6)	15.7 (0.6)	4.1 (0.8)
R_{sym} [b] (%) [a]	19.0 (>100)	14.0 (>100)	28.1 (>100)
R_{pim} [b] (%) [a]	10.8 (83.6)	5.9 (78.0)	11.5 (48.0)
$CC_{1/2}$ [c] (%) [a]	93 (39)	98 (34)	98 (34)
Refinement statistics			
Resolution (Å)	33.0-2.70	30.5-2.32	45.3-2.70
Reflections (work)	103,168	85,315	177,888
Reflections (test)	5237	4299	9028
R_{cryst} [d] / R_{free} [e] (%)	21.2/26.7	21.3/25.6	21.6/25.6
No. of copies in ASU	6	3	9
No. of atoms	23,751	12,264	36,829
HA	23,522	11,874	35,697
Glycans	187	56	525
Receptor analog		193	342
Solvent	42	141	265
Average *B*-values (Å^2)	85	82	53
HA	84	82	52
Glycans	106	74	70
Receptor analog		89	79
Solvent	60	60	37
Wilson *B*-value (Å^2)	68	59	42
RMSD from ideal geometry			
Bond length (Å)	0.003	0.003	0.003
Bond angle (°)	0.55	0.65	0.58
Ramachandran statistics (%) [f]			
Favored	96.0	97.6	96.8
Outliers	0.2	0.2	0.1
PDB code	9DIQ	9DIP	9DIO

Numbers in parentheses refer to the highest resolution shell.
[b] $R_{sym} = \Sigma_{hkl} \Sigma_i | I_{hkl,i} - <I_{hkl}> | / \Sigma_{hkl} \Sigma_i I_{hkl,i}$ and $R_{pim} = \Sigma_{hkl} (1/(n-1))^{1/2} \Sigma_i | I_{hkl,i} - <I_{hkl}> | / \Sigma_{hkl} \Sigma_i I_{hkl,i}$, where $I_{hkl,i}$ is the scaled intensity of the i^{th} measurement of reflection h, k, l, $<I_{hkl}>$ is the average intensity for that reflection, and *n* is the redundancy.
[c] $CC_{1/2}$ = Pearson correlation coefficient between two random half datasets.
[d] $R_{cryst} = \Sigma_{hkl} | F_o - F_c | / \Sigma_{hkl} | F_o |$ x 100, where F_o and F_c are the observed and calculated structure factors, respectively.
[e] R_{free} was calculated as for R_{cryst}, but on a test set comprising 5% or 10% of the data excluded from refinement.
[f] From MolProbity (*84*).

Table S2. List of glycans on glycan array

Chart#	Structure	Name
1	Galβ(1-4)-GlcNAcβ-ethyl-NH_2	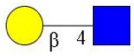
2	Galβ(1-4)-GlcNAcβ(1-2)-Manα(1-3)-[Galβ(1-4)-GlcNAcβ(1-2)-Manα(1-6)]-Manβ(1-4)-GlcNAcβ(1-4)-GlcNAcβ-Asn-NH_2	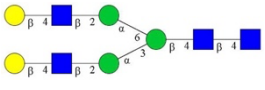
3	NeuAcα(2-3)-Galβ(1-4)-GlcNAcβ-ethyl-NH_2	
4	NeuAcα(2-3)-Galβ(1-4)-GlcNAcβ(1-3)-Galβ(1-4)-GlcNAcβ-ethyl-NH_2	
5	NeuAcα(2-3)-Galβ(1-4)-GlcNAcβ(1-3)-Galβ(1-4)-GlcNAcβ(1-3)-Galβ(1-4)-GlcNAcβ-ethyl-NH_2	
6	NeuAcα(2-3)-Galβ(1-3)-GalNAcα-Thr-NH_2	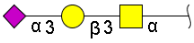
7	3' NeuAc LN Core 1 (1163)	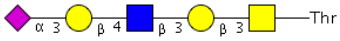

8	3' NeuAc DiLN Core 1 (1528)	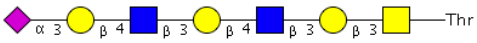
9	3' NeuAc TetraLN Core 1 (2259)	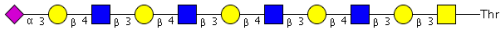
10	3' NeuAc PentaLN Core 1 (2624)	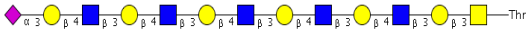
11	NeuAcα(2-3)-Galβ(1-4)-GlcNAcβ(1-6)-[Galβ(1-3)]-GalNAcα-Thr-NH_2	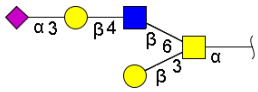
12	NeuAcα(2-3)-Galβ(1-4)-GlcNAcβ(1-3)-Galβ(1-4)-GlcNAcβ(1-6)-[Galβ(1-3)]-GalNAcα-Thr-NH_2	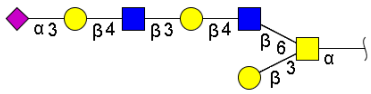
13	3' NeuAc TriLN Core 2 (1894)	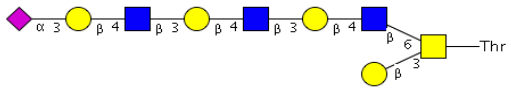
14	3' NeuAc TetraLN Core 2 (2259)	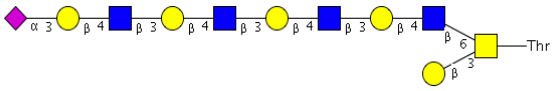
15	3' NeuAc PentaLN Core 2 (2624)	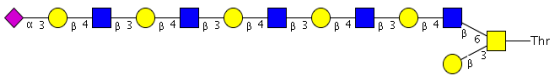

16	NeuAcα2-3Galβ1-4GlcNAcβ1-2Manα1-3(NeuAcα2-3Galβ1-4GlcNAcβ1-2Manα1-6)Manβ1-4GlcNAcβ1-4GlcNAc-AsnGly-NH_2	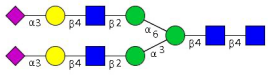
17	NeuAcα2-3Galβ1-4GlcNAcβ1-3Galβ1-4GlcNAcβ1-2Manα1-3(NeuAcα2-3Galβ1-4GlcNAcβ1-3Galβ1-4GlcNAcβ1-2Manα1-6)Manβ1-4GlcNAcβ1-4GlcNAc-AsnGly-NH_2	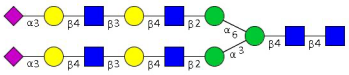
18	(NeuAcα2-3Galβ1-4GlcNAcβ1-3Galβ1-4GlcNAcβ1-3Galβ1-4GlcNAcβ1-2Manα1-6)NeuAcα2-3Galβ1-4GlcNAcβ1-3Galβ1-4GlcNAcβ1-3Galβ1-4GlcNAcβ1-2Manα1-3Manβ1-4GlcNAcβ1-4GlcNAc-AsnGly-NH_2	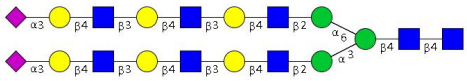
19	NeuAcα2-3Galβ1-4GlcNAcβ1-2Manα1-3(NeuAcα2-3Galβ1-4GlcNAcβ1-2Manα1-6)Manβ1-4GlcNAcβ1-4(Fucα1-6)GlcNAc-AsnGly-NH_2	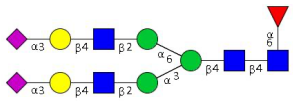
20	NeuAcα2-3Galβ1-4GlcNAcβ1-3Galβ1-4GlcNAcβ1-2Manα1-3(NeuAcα2-3Galβ1-4GlcNAcβ1-3Galβ1-4GlcNAcβ1-2Manα1-6)Manβ1-4GlcNAcβ1-4(Fucα1-6)GlcNAc-AsnGly-NH_2	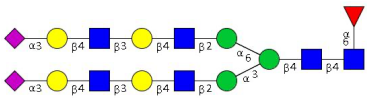
21	NeuAcα2-3Galβ1-4GlcNAcβ1-3Galβ1-4GlcNAcβ1-3Galβ1-4GlcNAcβ1-2Manα1-3(NeuAcα2-3Galβ1-4GlcNAcβ1-3Galβ1-4GlcNAcβ1-3Galβ1-4GlcNAcβ1-2Manα1-6)Manβ1-4GlcNAcβ1-4GlcNAc-AsnGly-NH_2	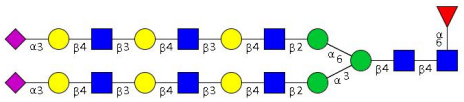
22	NeuAcα(2-3)-Galβ(1-4)-[Fucα(1-3)]-GlcNAcβ-propyl-NH_2	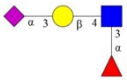
23	NeuAcα(2-3)-Galβ(1-4)-[Fucα(1-3)]-GlcNAcβ(1-3)-Galβ(1-4)-[Fucα(1-3)]-GlcNAcβ-ethyl-NH_2	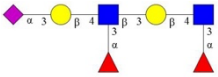

24	NeuAcα(2-3)-Galβ(1-4)-[Fucα(1-3)]-GlcNAcβ(1-3)-Galβ(1-4)-[Fucα(1-3)]-GlcNAcβ(1-3)-Galβ(1-4)-[Fucα(1-3)]-GlcNAcβ-ethyl-NH_2	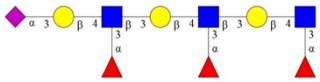
25	3' SLeX TriLN Core 1(2332)	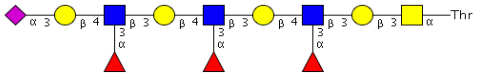
26	3' SLeX TriLN Core 3(2170)	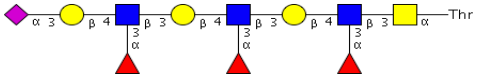
27	NeuAcα(2-6)-Galβ(1-4)-(6S)GlcNacβ-ethyl-NH_2	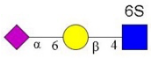
28	NeuAcα(2-6)-Galβ(1-4)-6-O-sulfo-GlcNAcβ-propyl-NH_2	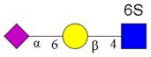
29	NeuAcα(2-6)-Galβ(1-4)-GlcNAcβ-ethyl-NH_2	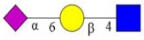
30	NeuAcα(2-6)-Galβ(1-4)-GlcNAcβ(1-3)-Galβ(1-4)-GlcNAcβ-ethyl-NH_2	
31	NeuAcα(2-6)-Galβ(1-4)-GlcNAcβ(1-3)-Galβ(1-4)-GlcNAcβ(1-3)-Galβ(1-4)-GlcNAcβ-ethyl-NH_2	

32	6' NeuAc LN Core 1 (1163)	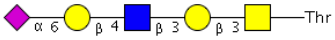
33	6' NeuAc DiLN Core 1 (1528)	
34	6' NeuAc TriLN Core 1 (1894)	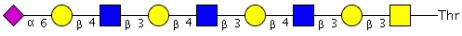
35	6' NeuAc TetraLN Core 1 (2259)	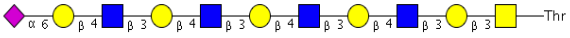
36	NeuAcα(2-6)-Galβ(1-4)-GlcNAcβ(1-6)-[Galβ(1-3)]-GalNAcα-Thr-NH_2	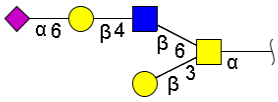
37	NeuAcα(2-6)-Galβ(1-4)-GlcNAcβ(1-3)-Galβ(1-4)-GlcNAcβ(1-6)-[Galβ(1-3)]-GalNAcα-Thr-NH_2	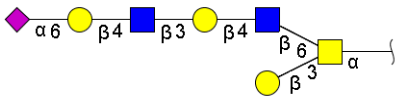
38	6' NeuAc TriLN Core 2 (1894)	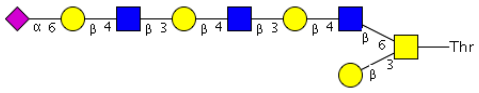
39	6' NeuAc TetraLN Core 2 (2259)	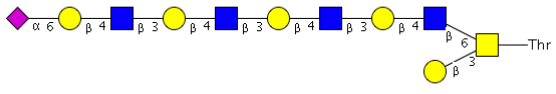

40	6' NeuAc PentaLN Core 2 (2624)	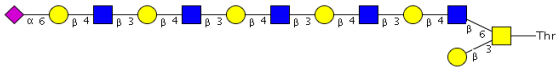
41	NeuAcα2-6Galβ1-4GlcNAcβ1-2Manα1-3(NeuAcα2-6Galβ1-4GlcNAcβ1-2Manα1-6)Manβ1-4GlcNAcβ1-4GlcNAc-AsnGly	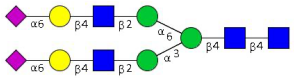
42	NeuAcα2-6Galβ1-4GlcNAcβ1-3Galβ1-4GlcNAcβ1-2Manα1-3(NeuAcα2-6Galβ1-4GlcNAcβ1-3Galβ1-4GlcNAcβ1-2Manα1-6)Manβ1-4GlcNAcβ1-4GlcNAc-AsnGly	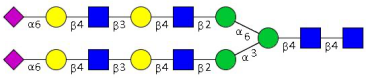
43	NeuAcα2-6Galβ1-4GlcNAcβ1-3Galβ1-4GlcNAcβ1-3Galβ1-4GlcNAcβ1-2Manα1-3(NeuAcα2-6Galβ1-4GlcNAcβ1-3Galβ1-4GlcNAcβ1-3Galβ1-4GlcNAcβ1-2Manα1-6)Manβ1-4GlcNAcβ1-4GlcNAc-AsnGly	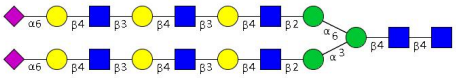
44	NeuAcα2-6Galβ1-4GlcNAcβ1-2Manα1-3(NeuAcα2-6Galβ1-4GlcNAcβ1-2Manα1-6)Manβ1-4GlcNAcβ1-4(Fucα1-6)GlcNAc-AsnGly	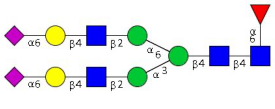
45	NeuAcα2-6Galβ1-4GlcNAcβ1-3Galβ1-4GlcNAcβ1-2Manα1-3(NeuAcα2-6Galβ1-4GlcNAcβ1-3Galβ1-4GlcNAcβ1-2Manα1-6)Manβ1-4GlcNAcβ1-4(Fucα1-6)GlcNAc-AsnGly	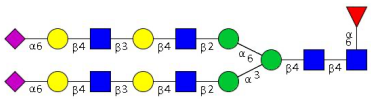
46	NeuAcα2-6Galβ1-4GlcNAcβ1-3Galβ1-4GlcNAcβ1-3Galβ1-4GlcNAcβ1-2Manα1-3(NeuAcα2-6Galβ1-4GlcNAcβ1-3Galβ1-4GlcNAcβ1-3Galβ1-4GlcNAcβ1-2Manα1-6)Manβ1-4GlcNAcβ1-4GlcNAc-AsnGly	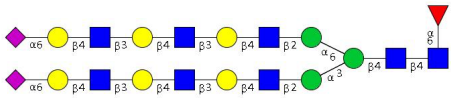

References and Notes

1. X. Xu, N. J. Subbarao, N. J. Cox, Y. Guo, Genetic characterization of the pathogenic influenza A/Goose/Guangdong/1/96 (H5N1) virus: Similarity of its hemagglutinin gene to those of H5N1 viruses from the 1997 outbreaks in Hong Kong. *Virology* **261**, 15–19 (1999). doi:10.1006/viro.1999.9820 Medline

2. A. Fusaro, B. Zecchin, E. Giussani, E. Palumbo, M. Agüero-García, C. Bachofen, Á. Bálint, F. Banihashem, A. C. Banyard, N. Beerens, M. Bourg, F.-X. Briand, C. Bröjer, I. H. Brown, B. Brugger, A. M. P. Byrne, A. Cana, V. Christodoulou, Z. Dirbakova, T. Fagulha, R. A. M. Fouchier, L. Garza-Cuartero, G. Georgiades, B. Gjerset, B. Grasland, O. Groza, T. Harder, A. M. Henriques, C. K. Hjulsager, E. Ivanova, Z. Janeliunas, L. Krivko, K. Lemon, Y. Liang, A. Lika, P. Malik, M. J. McMenamy, A. Nagy, I. Nurmoja, I. Onita, A. Pohlmann, S. Revilla-Fernández, A. Sánchez-Sánchez, V. Savic, B. Slavec, K. Smietanka, C. J. Snoeck, M. Steensels, V. Svansson, E. Swieton, N. Tammiranta, M. Tinak, S. Van Borm, S. Zohari, C. Adlhoch, F. Baldinelli, C. Terregino, I. Monne, High pathogenic avian influenza A(H5) viruses of clade 2.3.4.4b in Europe-Why trends of virus evolution are more difficult to predict. *Virus Evol.* **10**, veae027 (2024). doi:10.1093/ve/veae027 Medline

3. B. Olsen, V. J. Munster, A. Wallensten, J. Waldenström, A. D. M. E. Osterhaus, R. A. M. Fouchier, Global patterns of influenza a virus in wild birds. *Science* **312**, 384–388 (2006). doi:10.1126/science.1122438 Medline

4. A. Fusaro, B. Zecchin, B. Vrancken, C. Abolnik, R. Ademun, A. Alassane, A. Arafa, J. A. Awuni, E. Couacy-Hymann, M. B. Coulibaly, N. Gaidet, E. Go-Maro, T. Joannis, S. D. Jumbo, G. Minoungou, C. Meseko, M. M. Souley, D. B. Ndumu, I. Shittu, A. Twabela, A. Wade, L. Wiersma, Y. P. Akpeli, G. Zamperin, A. Milani, P. Lemey, I. Monne, Disentangling the role of Africa in the global spread of H5 highly pathogenic avian influenza. *Nat. Commun.* **10**, 5310 (2019). doi:10.1038/s41467-019-13287-y Medline

5. M. Engelsma, R. Heutink, F. Harders, E. A. Germeraad, N. Beerens, Multiple introductions of reassorted highly pathogenic avian influenza H5Nx viruses clade 2.3.4.4b causing outbreaks in wild birds and poultry in the Netherlands, 2020-2021. *Microbiol. Spectr.* **10**, e0249921 (2022). doi:10.1128/spectrum.02499-21 Medline

6. S. Lin, J. Chen, K. Li, Y. Liu, S. Fu, S. Xie, A. Zha, A. Xin, X. Han, Y. Shi, L. Xu, M. Liao, W. Jia, Evolutionary dynamics and comparative pathogenicity of clade 2.3.4.4b H5 subtype avian influenza viruses, China, 2021-2022. *Virol. Sin.* **39**, 358–368 (2024). doi:10.1016/j.virs.2024.04.004 Medline

7. G. J. Smith, R. O. Donis; World Health Organization/World Organisation for Animal Health/Food and Agriculture Organization (WHO/OIE/FAO) H5 Evolution Working Group, Nomenclature updates resulting from the evolution of avian influenza A(H5) virus clades

2.1.3.2a, 2.2.1, and 2.3.4 during 2013-2014. *Influenza Other Respir. Viruses* **9**, 271–276 (2015). doi:10.1111/irv.12324 Medline

8. M. Sagong, Y.-N. Lee, S. Song, R. M. Cha, E.-K. Lee, Y.-M. Kang, H.-K. Cho, H.-M. Kang, Y.-J. Lee, K.-N. Lee, Emergence of clade 2.3.4.4b novel reassortant H5N1 high pathogenicity avian influenza virus in South Korea during late 2021. *Transbound. Emerg. Dis.* **69**, e3255–e3260 (2022). doi:10.1111/tbed.14551 Medline

9. V. Caliendo, N. S. Lewis, A. Pohlmann, S. R. Baillie, A. C. Banyard, M. Beer, I. H. Brown, R. A. M. Fouchier, R. D. E. Hansen, T. K. Lameris, A. S. Lang, S. Laurendeau, O. Lung, G. Robertson, H. van der Jeugd, T. N. Alkie, K. Thorup, M. L. van Toor, J. Waldenström, C. Yason, T. Kuiken, Y. Berhane, Transatlantic spread of highly pathogenic avian influenza H5N1 by wild birds from Europe to North America in 2021. *Sci. Rep.* **12**, 11729 (2022). doi:10.1038/s41598-022-13447-z Medline

10. S. N. Bevins, S. A. Shriner, J. C. Cumbee Jr., K. E. Dilione, K. E. Douglass, J. W. Ellis, M. L. Killian, M. K. Torchetti, J. B. Lenoch, Intercontinental movement of highly pathogenic avian influenza A(H5N1) clade 2.3.4.4 virus to the United States, 2021. *Emerg. Infect. Dis.* **28**, 1006–1011 (2022). doi:10.3201/eid2805.220318 Medline

11. S. Youk, M. K. Torchetti, K. Lantz, J. B. Lenoch, M. L. Killian, C. Leyson, S. N. Bevins, K. Dilione, H. S. Ip, D. E. Stallknecht, R. L. Poulson, D. L. Suarez, D. E. Swayne, M. J. Pantin-Jackwood, H5N1 highly pathogenic avian influenza clade 2.3.4.4b in wild and domestic birds: Introductions into the United States and reassortments, December 2021-April 2022. *Virology* **587**, 109860 (2023). doi:10.1016/j.virol.2023.109860 Medline

12. E. J. Elsmo, A. Wünschmann, K. B. Beckmen, L. E. Broughton-Neiswanger, E. L. Buckles, J. Ellis, S. D. Fitzgerald, R. Gerlach, S. Hawkins, H. S. Ip, J. S. Lankton, E. M. Lemley, J. B. Lenoch, M. L. Killian, K. Lantz, L. Long, R. Maes, M. Mainenti, J. Melotti, M. E. Moriarty, S. Nakagun, R. M. Ruden, V. Shearn-Bochsler, D. Thompson, M. K. Torchetti, A. J. Van Wettere, A. G. Wise, A. L. Lim, Highly pathogenic avian influenza A(H5N1) virus clade 2.3.4.4b infections in wild terrestrial mammals, United States, 2022. *Emerg. Infect. Dis.* **29**, 2451–2460 (2023). doi:10.3201/eid2912.230464 Medline

13. G. Graziosi, C. Lupini, E. Catelli, S. Carnaccini, Highly pathogenic avian influenza (HPAI) H5 clade 2.3.4.4b virus infection in birds and mammals. *Animals (Basel)* **14**, 1372 (2024). doi:10.3390/ani14091372 Medline

14. B. D. Cronk, L. C. Caserta, M. Laverack, R. S. Gerdes, K. Hynes, C. R. Hopf, M. A. Fadden, S. Nakagun, K. L. Schuler, E. L. Buckles, M. Lejeune, D. G. Diel, Infection and tissue distribution of highly pathogenic avian influenza A type H5N1 (clade 2.3.4.4b) in red fox kits (*Vulpes vulpes*). *Emerg. Microbes Infect.* **12**, 2249554 (2023). doi:10.1080/22221751.2023.2249554 Medline

15. J. D. Brown, A. Black, K. H. Haman, D. G. Diel, V. E. Ramirez, R. S. Ziejka, H. T. Fenelon, P. M. Rabinowitz, L. Stevens, R. Poulson, D. E. Stallknecht, Antibodies to influenza A(H5N1) virus in hunting dogs retrieving wild fowl, Washington, USA. *Emerg. Infect. Dis.* **30**, 1271–1274 (2024). doi:10.3201/eid3006.231459 Medline

16. M. Falchieri, S. M. Reid, A. Dastderji, J. Cracknell, C. J. Warren, B. C. Mollett, J. Peers-Dent, A. D. Schlachter, N. Mcginn, R. Hepple, S. Thomas, S. Ridout, J. Quayle, R. Pizzi, A. Núñez, A. M. P. Byrne, J. James, A. C. Banyard, Rapid mortality in captive bush dogs (*Speothos venaticus*) caused by influenza A of avian origin (H5N1) at a wildlife collection in the United Kingdom. *Emerg. Microbes Infect.* **13**, 2361792 (2024). doi:10.1080/22221751.2024.2361792 Medline

17. J. A. Pulit-Penaloza, N. Brock, J. A. Belser, X. Sun, C. Pappas, T. J. Kieran, P. Basu Thakur, H. Zeng, D. Cui, J. Frederick, R. Fasce, T. M. Tumpey, T. R. Maines, Highly pathogenic avian influenza A(H5N1) virus of clade 2.3.4.4b isolated from a human case in Chile causes fatal disease and transmits between co-housed ferrets. *Emerg. Microbes Infect.* **13**, 2332667 (2024). doi:10.1080/22221751.2024.2332667 Medline

18. M. Agüero, I. Monne, A. Sánchez, B. Zecchin, A. Fusaro, M. J. Ruano, M. Del Valle Arrojo, R. Fernández-Antonio, A. M. Souto, P. Tordable, J. Cañás, F. Bonfante, E. Giussani, C. Terregino, J. J. Orejas, Highly pathogenic avian influenza A(H5N1) virus infection in farmed minks, Spain, October 2022. *Euro Surveill.* **28**, 2300001 (2023). doi:10.2807/1560-7917.ES.2023.28.3.2300001 Medline

19. S. J. Sillman, M. Drozd, D. Loy, S. P. Harris, Naturally occurring highly pathogenic avian influenza virus H5N1 clade 2.3.4.4b infection in three domestic cats in North America during 2023. *J. Comp. Pathol.* **205**, 17–23 (2023). doi:10.1016/j.jcpa.2023.07.001 Medline

20. E. R. Burrough, D. R. Magstadt, B. Petersen, S. J. Timmermans, P. C. Gauger, J. Zhang, C. Siepker, M. Mainenti, G. Li, A. C. Thompson, P. J. Gorden, P. J. Plummer, R. Main, Highly pathogenic avian influenza A(H5N1) clade 2.3.4.4b virus infection in domestic dairy cattle and cats, United States, 2024. *Emerg. Infect. Dis.* **30**, 1335–1343 (2024). doi:10.3201/eid3007.240508 Medline

21. A. Bruno, A. Alfaro-Núñez, D. de Mora, R. Armas, M. Olmedo, J. Garcés, M. A. Garcia-Bereguiain, First case of human infection with highly pathogenic H5 avian Influenza A virus in South America: A new zoonotic pandemic threat for 2023? *J. Travel Med.* **30**, taad032 (2023). doi:10.1093/jtm/taad032 Medline

22. S. Lair, L. Quesnel, A. V. Signore, P. Delnatte, C. Embury-Hyatt, M.-S. Nadeau, O. Lung, S. T. Ferrell, R. Michaud, Y. Berhane, Outbreak of highly pathogenic avian Influenza A(H5N1) virus in seals, St. Lawrence Estuary, Quebec, Canada. *Emerg. Infect. Dis.* **30**, 1133–1143 (2024). doi:10.3201/eid3006.231033 Medline

23. M. Leguia, A. Garcia-Glaessner, B. Muñoz-Saavedra, D. Juarez, P. Barrera, C. Calvo-Mac, J. Jara, W. Silva, K. Ploog, L. Amaro, P. Colchao-Claux, C. K. Johnson, M. M. Uhart, M. I. Nelson, J. Lescano, Highly pathogenic avian influenza A (H5N1) in marine mammals and seabirds in Peru. *Nat. Commun.* **14**, 5489 (2023). doi:10.1038/s41467-023-41182-0 Medline

24. P. I. Plaza, V. Gamarra-Toledo, J. Rodríguez Euguí, N. Rosciano, S. A. Lambertucci, Pacific and Atlantic sea lion mortality caused by highly pathogenic Avian Influenza A(H5N1) in South America. *Travel Med. Infect. Dis.* **59**, 102712 (2024). doi:10.1016/j.tmaid.2024.102712 Medline

25. M. Uhart *et al*., Massive outbreak of Influenza A H5N1 in elephant seals at Península Valdés, Argentina: increased evidence for mammal-to-mammal transmission. *bioRxiv* (2024); https://www.biorxiv.org/content/10.1101/2024.05.31.596774v1.

26. T. M. Uyeki, S. Milton, C. Abdul Hamid, C. Reinoso Webb, S. M. Presley, V. Shetty, S. N. Rollo, D. L. Martinez, S. Rai, E. R. Gonzales, K. L. Kniss, Y. Jang, J. C. Frederick, J. A. De La Cruz, J. Liddell, H. Di, M. K. Kirby, J. R. Barnes, C. T. Davis, Highly pathogenic avian Influenza A(H5N1) virus infection in a dairy farm worker. *N. Engl. J. Med.* **390**, 2028–2029 (2024). doi:10.1056/NEJMc2405371 Medline

27. Centers for Disease Control and Prevention, Current H5N1 bird flu situation in dairy cows, 2024; https://www.cdc.gov/bird-flu/situation-summary/mammals.html

28. L. C. Caserta, E. A. Frye, S. L. Butt, M. Laverack, M. Nooruzzaman, L. M. Covaleda, A. C. Thompson, M. P. Koscielny, B. Cronk, A. Johnson, K. Kleinhenz, E. E. Edwards, G. Gomez, G. Hitchener, M. Martins, D. R. Kapczynski, D. L. Suarez, E. R. Alexander Morris, T. Hensley, J. S. Beeby, M. Lejeune, A. K. Swinford, F. Elvinger, K. M. Dimitrov, D. G. Diel, Spillover of highly pathogenic avian influenza H5N1 virus to dairy cattle. *Nature* **634**, 669–676 (2024). doi:10.1038/s41586-024-07849-4 Medline

29. Centers for Disease Control and Prevention, Technical report: June 2024 Highly pathogenic avian influenza A(H5N1) viruses (2024); https://www.cdc.gov/bird-flu/php/technical-report/h5n1-06052024.html.

30. Centers for Disease Control and Prevention, H5 bird flu: current situation, (2024); https://www.cdc.gov/bird-flu/situation-summary/index.html?CDC_AA_refVal=https%3A%2F%2Fwww.cdc.gov%2Fflu%2Favianflu%2Favian-flu-summary.htm.

31. C. C. Drehoff, E. B. White, A. M. Frutos, G. Stringer, A. Burakoff, N. Comstock, A. Cronquist, N. Alden, I. Armistead, A. Kohnen, R. Ratnabalasuriar, E. A. Travanty, S. R. Matzinger, A. Rossheim, A. Wellbrock, H. P. Pagano, D. Wang, J. Singleton, R. A. Sutter, C. T. Davis, K. Kniss, S. Ellington, M. K. Kirby, C. Reed, R. Herlihy; H5N1 Field Investigation Team, Cluster of influenza A(H5) cases associated with poultry exposure at two facilities -

Colorado, July 2024. *MMWR Morb. Mortal. Wkly. Rep.* **73**, 734–739 (2024). doi:10.15585/mmwr.mm7334a1 Medline

32. World Health Organization, Cumulative number of confirmed human cases of avian influenza A(H5N1) reported to WHO (2024); https://www.who.int/publications/m/item/cumulative-number-of-confirmed-human-cases-for-avian-influenza-a(h5n1)-reported-to-who--2003-2024--27-september-2024.

33. T. M. Tumpey, T. R. Maines, N. Van Hoeven, L. Glaser, A. Solórzano, C. Pappas, N. J. Cox, D. E. Swayne, P. Palese, J. M. Katz, A. García-Sastre, A two-amino acid change in the hemagglutinin of the 1918 influenza virus abolishes transmission. *Science* **315**, 655–659 (2007). doi:10.1126/science.1136212 Medline

34. K. Shinya, M. Ebina, S. Yamada, M. Ono, N. Kasai, Y. Kawaoka, Influenza virus receptors in the human airway. *Nature* **440**, 435–436 (2006). doi:10.1038/440435a Medline

35. N. J. Cox, S. C. Trock, S. A. Burke, Pandemic preparedness and the Influenza Risk Assessment Tool (IRAT). *Curr. Top. Microbiol. Immunol.* **385**, 119–136 (2014). doi:10.1007/82_2014_419 Medline

36. A. Jayaraman, C. Pappas, R. Raman, J. A. Belser, K. Viswanathan, Z. Shriver, T. M. Tumpey, R. Sasisekharan, A single base-pair change in 2009 H1N1 hemagglutinin increases human receptor affinity and leads to efficient airborne viral transmission in ferrets. *PLOS ONE* **6**, e17616 (2011). doi:10.1371/journal.pone.0017616 Medline

37. A. J. Thompson, J. C. Paulson, Adaptation of influenza viruses to human airway receptors. *J. Biol. Chem.* **296**, 100017 (2021). doi:10.1074/jbc.REV120.013309 Medline

38. L. Glaser, J. Stevens, D. Zamarin, I. A. Wilson, A. García-Sastre, T. M. Tumpey, C. F. Basler, J. K. Taubenberger, P. Palese, A single amino acid substitution in 1918 influenza virus hemagglutinin changes receptor binding specificity. *J. Virol.* **79**, 11533–11536 (2005). doi:10.1128/JVI.79.17.11533-11536.2005 Medline

39. G. N. Rogers, J. C. Paulson, R. S. Daniels, J. J. Skehel, I. A. Wilson, D. C. Wiley, Single amino acid substitutions in influenza haemagglutinin change receptor binding specificity. *Nature* **304**, 76–78 (1983). doi:10.1038/304076a0 Medline

40. Y. Liu, R. A. Childs, T. Matrosovich, S. Wharton, A. S. Palma, W. Chai, R. Daniels, V. Gregory, J. Uhlendorff, M. Kiso, H.-D. Klenk, A. Hay, T. Feizi, M. Matrosovich, Altered receptor specificity and cell tropism of D222G hemagglutinin mutants isolated from fatal cases of pandemic A(H1N1) 2009 influenza virus. *J. Virol.* **84**, 12069–12074 (2010). doi:10.1128/JVI.01639-10 Medline

41. A. H. Reid, T. A. Janczewski, R. M. Lourens, A. J. Elliot, R. S. Daniels, C. L. Berry, J. S. Oxford, J. K. Taubenberger, 1918 influenza pandemic caused by highly conserved viruses

with two receptor-binding variants. *Emerg. Infect. Dis.* **9**, 1249–1253 (2003). doi:10.3201/eid0910.020789 Medline

42. J. Stevens, O. Blixt, T. M. Tumpey, J. K. Taubenberger, J. C. Paulson, I. A. Wilson, Structure and receptor specificity of the hemagglutinin from an H5N1 influenza virus. *Science* **312**, 404–410 (2006). doi:10.1126/science.1124513 Medline

43. W. Zhang, Y. Shi, X. Lu, Y. Shu, J. Qi, G. F. Gao, An airborne transmissible avian influenza H5 hemagglutinin seen at the atomic level. *Science* **340**, 1463–1467 (2013). doi:10.1126/science.1236787 Medline

44. J. Stevens, O. Blixt, L.-M. Chen, R. O. Donis, J. C. Paulson, I. A. Wilson, Recent avian H5N1 viruses exhibit increased propensity for acquiring human receptor specificity. *J. Mol. Biol.* **381**, 1382–1394 (2008). doi:10.1016/j.jmb.2008.04.016 Medline

45. J. C. Paulson, R. P. de Vries, H5N1 receptor specificity as a factor in pandemic risk. *Virus Res.* **178**, 99–113 (2013). doi:10.1016/j.virusres.2013.02.015 Medline

46. S. Chutinimitkul, D. van Riel, V. J. Munster, J. M. A. van den Brand, G. F. Rimmelzwaan, T. Kuiken, A. D. M. E. Osterhaus, R. A. M. Fouchier, E. de Wit, In vitro assessment of attachment pattern and replication efficiency of H5N1 influenza A viruses with altered receptor specificity. *J. Virol.* **84**, 6825–6833 (2010). doi:10.1128/JVI.02737-09 Medline

47. D. Eggink, M. Spronken, R. van der Woude, J. Buzink, F. Broszeit, R. McBride, H. A. Pawestri, V. Setiawaty, J. C. Paulson, G.-J. Boons, R. A. M. Fouchier, C. A. Russell, M. D. de Jong, R. P. de Vries, Phenotypic effects of substitutions within the receptor binding site of highly pathogenic avian influenza H5N1 virus observed during human infection. *J. Virol.* **94**, e00195–e00120 (2020). doi:10.1128/JVI.00195-20 Medline

48. B. Dadonaite, J. J. Ahn, J. T. Ort, J. Yu, C. Furey, A. Dosey, W. W. Hannon, A. L. Vincent Baker, R. J. Webby, N. P. King, Y. Liu, S. E. Hensley, T. P. Peacock, L. H. Moncla, J. D. Bloom, Deep mutational scanning of H5 hemagglutinin to inform influenza virus surveillance. *PLOS Biol.* **22**, e3002916 (2024).

49. M. Imai, T. Watanabe, M. Hatta, S. C. Das, M. Ozawa, K. Shinya, G. Zhong, A. Hanson, H. Katsura, S. Watanabe, C. Li, E. Kawakami, S. Yamada, M. Kiso, Y. Suzuki, E. A. Maher, G. Neumann, Y. Kawaoka, Experimental adaptation of an influenza H5 HA confers respiratory droplet transmission to a reassortant H5 HA/H1N1 virus in ferrets. *Nature* **486**, 420–428 (2012). doi:10.1038/nature10831 Medline

50. S. Herfst, E. J. A. Schrauwen, M. Linster, S. Chutinimitkul, E. de Wit, V. J. Munster, E. M. Sorrell, T. M. Bestebroer, D. F. Burke, D. J. Smith, G. F. Rimmelzwaan, A. D. M. E. Osterhaus, R. A. M. Fouchier, Airborne transmission of influenza A/H5N1 virus between ferrets. *Science* **336**, 1534–1541 (2012). doi:10.1126/science.1213362 Medline

51. P. Chopra *et al*., Receptor binding specificity of a bovine A(H5N1) influenza virus. *bioRxiv* (2024); https://www.biorxiv.org/content/10.1101/2024.07.30.605893v1.

52. J. J. S. Santos *et al*., Bovine H5N1 influenza virus binds poorly to human-type sialic acid receptors. *bioRxiv* (2024); https://www.biorxiv.org/content/10.1101/2024.08.01.606177v1.

53. W. Peng, K. M. Bouwman, R. McBride, O. C. Grant, R. J. Woods, M. H. Verheije, J. C. Paulson, R. P. de Vries, Enhanced human-type receptor binding by ferret-transmissible H5N1 with a K193T mutation. *J. Virol.* **92**, e02016–e02017 (2018). doi:10.1128/JVI.02016-17 Medline

54. L. M. Chen, O. Blixt, J. Stevens, A. S. Lipatov, C. T. Davis, B. E. Collins, N. J. Cox, J. C. Paulson, R. O. Donis, In vitro evolution of H5N1 avian influenza virus toward human-type receptor specificity. *Virology* **422**, 105–113 (2012). doi:10.1016/j.virol.2011.10.006 Medline

55. R. P. de Vries, W. Peng, O. C. Grant, A. J. Thompson, X. Zhu, K. M. Bouwman, A. T. T. de la Pena, M. J. van Breemen, I. N. Ambepitiya Wickramasinghe, C. A. M. de Haan, W. Yu, R. McBride, R. W. Sanders, R. J. Woods, M. H. Verheije, I. A. Wilson, J. C. Paulson, Three mutations switch H7N9 influenza to human-type receptor specificity. *PLOS Pathog.* **13**, e1006390 (2017). doi:10.1371/journal.ppat.1006390 Medline

56. M. B. Eisen, S. Sabesan, J. J. Skehel, D. C. Wiley, Binding of the influenza A virus to cell-surface receptors: Structures of five hemagglutinin-sialyloligosaccharide complexes determined by X-ray crystallography. *Virology* **232**, 19–31 (1997). doi:10.1006/viro.1997.8526 Medline

57. M. Crusat, J. Liu, A. S. Palma, R. A. Childs, Y. Liu, S. A. Wharton, Y. P. Lin, P. J. Coombs, S. R. Martin, M. Matrosovich, Z. Chen, D. J. Stevens, V. M. Hien, T. T. Thanh, N. T. Nhu, L. A. Nguyet, Q. Ha, H. R. van Doorn, T. T. Hien, H. S. Conradt, M. Kiso, S. J. Gamblin, W. Chai, J. J. Skehel, A. J. Hay, J. Farrar, M. D. de Jong, T. Feizi, Changes in the hemagglutinin of H5N1 viruses during human infection—Influence on receptor binding. *Virology* **447**, 326–337 (2013). doi:10.1016/j.virol.2013.08.010 Medline

58. K. Tharakaraman, R. Raman, K. Viswanathan, N. W. Stebbins, A. Jayaraman, A. Krishnan, V. Sasisekharan, R. Sasisekharan, Structural determinants for naturally evolving H5N1 hemagglutinin to switch its receptor specificity. *Cell* **153**, 1475–1485 (2013). doi:10.1016/j.cell.2013.05.035 Medline

59. X. Zhu, K. Viswanathan, R. Raman, W. Yu, R. Sasisekharan, I. A. Wilson, Structural basis for a switch in receptor binding specificity of two H5N1 hemagglutinin mutants. *Cell Rep.* **13**, 1683–1691 (2015). doi:10.1016/j.celrep.2015.10.027 Medline

60. J. Liu, D. J. Stevens, L. F. Haire, P. A. Walker, P. J. Coombs, R. J. Russell, S. J. Gamblin, J. J. Skehel, Structures of receptor complexes formed by hemagglutinins from the Asian Influenza

pandemic of 1957. *Proc. Natl. Acad. Sci. U.S.A.* **106**, 17175–17180 (2009). doi:10.1073/pnas.0906849106 Medline

61. J. Yang *et al*., The haemagglutinin gene of bovine origin H5N1 influenza viruses currently retains an avian influenza virus phenotype. *bioRxiv* (2024); https://www.biorxiv.org/content/10.1101/2024.09.27.615407v1.

62. M. R. Good, W. Ji, M. L. Fernández-Quintero, A. B. Ward, J. J. Guthmiller, A single mutation in dairy cow-associated H5N1 viruses increases receptor binding breadth. *bioRxiv* (2024); https://www.biorxiv.org/content/10.1101/2024.06.22.600211v1.

63. A. J. Eisfeld, A. Biswas, L. Guan, C. Gu, T. Maemura, S. Trifkovic, T. Wang, L. Babujee, R. Dahn, P. J. Halfmann, T. Barnhardt, G. Neumann, Y. Suzuki, A. Thompson, A. K. Swinford, K. M. Dimitrov, K. Poulsen, Y. Kawaoka, Pathogenicity and transmissibility of bovine H5N1 influenza virus. *Nature* **633**, 426–432 (2024). doi:10.1038/s41586-024-07766-6 Medline

64. M. Imai, Y. Kawaoka, The role of receptor binding specificity in interspecies transmission of influenza viruses. *Curr. Opin. Virol.* **2**, 160–167 (2012). doi:10.1016/j.coviro.2012.03.003 Medline

65. C. Kristensen, H. E. Jensen, R. Trebbien, R. J. Webby, L. E. Larsen, Avian and Human influenza A virus receptors in bovine mammary gland. *Emerg. Infect. Dis.* **30**, 1907–1911 (2024). doi:10.3201/eid3009.240696 Medline

66. R. K. Nelli, T. A. Harm, C. Siepker, J. M. Groeltz-Thrush, B. Jones, N.-C. Twu, A. S. Nenninger, D. R. Magstadt, E. R. Burrough, P. E. Piñeyro, M. Mainenti, S. Carnaccini, P. J. Plummer, T. M. Bell, Sialic acid receptor specificity in mammary gland of dairy cattle infected with highly pathogenic avian influenza A(H5N1) virus. *Emerg. Infect. Dis.* **30**, 1361–1373 (2024). doi:10.3201/eid3007.240689 Medline

67. R. Xu, X. Zhu, R. McBride, C. M. Nycholat, W. Yu, J. C. Paulson, I. A. Wilson, Functional balance of the hemagglutinin and neuraminidase activities accompanies the emergence of the 2009 H1N1 influenza pandemic. *J. Virol.* **86**, 9221–9232 (2012). doi:10.1128/JVI.00697-12 Medline

68. A. Harris, G. Cardone, D. C. Winkler, J. B. Heymann, M. Brecher, J. M. White, A. C. Steven, Influenza virus pleiomorphy characterized by cryoelectron tomography. *Proc. Natl. Acad. Sci. U.S.A.* **103**, 19123–19127 (2006). doi:10.1073/pnas.0607614103 Medline

69. H. Zhang, X. Li, J. Guo, L. Li, C. Chang, Y. Li, C. Bian, K. Xu, H. Chen, B. Sun, The PB2 E627K mutation contributes to the high polymerase activity and enhanced replication of H7N9 influenza virus. *J. Gen. Virol.* **95**, 779–786 (2014). doi:10.1099/vir.0.061721-0 Medline

70. P. P. Petric, M. Schwemmle, L. Graf, Anti-influenza A virus restriction factors that shape the human species barrier and virus evolution. *PLOS Pathog.* **19**, e1011450 (2023). doi:10.1371/journal.ppat.1011450 Medline

71. J. Yang *et al*., The haemagglutinin genes of the UK clade 2.3.4.4b H5N1 avian influenza viruses from 2020 to 2022 retain strong avian phenotype. *bioRxiv* (2024); https://www.biorxiv.org/content/10.1101/2024.07.09.602706v1.

72. Y. Shtyrya, L. Mochalova, G. Voznova, I. Rudneva, A. Shilov, N. Kaverin, N. Bovin, Adjustment of receptor-binding and neuraminidase substrate specificities in avian-human reassortant influenza viruses. *Glycoconj. J.* **26**, 99–109 (2009). doi:10.1007/s10719-008-9169-x Medline

73. N. Le Briand, J. S. Casalegno, V. Escuret, A. Gaymard, B. Lina, M. Ottmann, E. Frobert, La balance HA-NA des virus influenza A(H1N1). *Virologie* **20**, 47–60 (2016). Medline

74. Y. Shu, J. McCauley, GISAID: Global initiative on sharing all influenza data - from vision to reality. *Euro Surveill.* **22**, 30494 (2017). doi:10.2807/1560-7917.ES.2017.22.13.30494 Medline

75. D. C. Ekiert, R. H. E. Friesen, G. Bhabha, T. Kwaks, M. Jongeneelen, W. Yu, C. Ophorst, F. Cox, H. J. W. M. Korse, B. Brandenburg, R. Vogels, J. P. J. Brakenhoff, R. Kompier, M. H. Koldijk, L. A. H. M. Cornelissen, L. L. M. Poon, M. Peiris, W. Koudstaal, I. A. Wilson, J. Goudsmit, A highly conserved neutralizing epitope on group 2 influenza A viruses. *Science* **333**, 843–850 (2011). doi:10.1126/science.1204839 Medline

76. R. P. de Vries, E. de Vries, B. J. Bosch, R. J. de Groot, P. J. M. Rottier, C. A. M. de Haan, The influenza A virus hemagglutinin glycosylation state affects receptor-binding specificity. *Virology* **403**, 17–25 (2010). doi:10.1016/j.virol.2010.03.047 Medline

77. X. Zhu, Y.-H. Guo, T. Jiang, Y.-D. Wang, K.-H. Chan, X.-F. Li, W. Yu, R. McBride, J. C. Paulson, K.-Y. Yuen, C.-F. Qin, X.-Y. Che, I. A. Wilson, A unique and conserved neutralization epitope in H5N1 influenza viruses identified by an antibody against the A/Goose/Guangdong/1/96 hemagglutinin. *J. Virol.* **87**, 12619–12635 (2013). doi:10.1128/JVI.01577-13 Medline

78. Z. Otwinowski, W. Minor, Processing of X-ray diffraction data collected in oscillation mode. *Methods Enzymol.* **276**, 307–326 (1997). doi:10.1016/S0076-6879(97)76066-X Medline

79. A. J. McCoy, R. W. Grosse-Kunstleve, P. D. Adams, M. D. Winn, L. C. Storoni, R. J. Read, Phaser crystallographic software. *J. Appl. Cryst.* **40**, 658–674 (2007). doi:10.1107/S0021889807021206 Medline

80. P. Emsley, B. Lohkamp, W. G. Scott, K. Cowtan, Features and development of Coot. *Acta Crystallogr. D Biol. Crystallogr.* **66**, 486–501 (2010). doi:10.1107/S0907444910007493 Medline

81. P. D. Adams, P. V. Afonine, G. Bunkóczi, V. B. Chen, I. W. Davis, N. Echols, J. J. Headd, L.-W. Hung, G. J. Kapral, R. W. Grosse-Kunstleve, A. J. McCoy, N. W. Moriarty, R. Oeffner, R. J. Read, D. C. Richardson, J. S. Richardson, T. C. Terwilliger, P. H. Zwart, PHENIX: A comprehensive Python-based system for macromolecular structure solution. *Acta Crystallogr. D Biol. Crystallogr.* **66**, 213–221 (2010). doi:10.1107/S0907444909052925 Medline

82. W. Peng, R. P. de Vries, O. C. Grant, A. J. Thompson, R. McBride, B. Tsogtbaatar, P. S. Lee, N. Razi, I. A. Wilson, R. J. Woods, J. C. Paulson, Recent H3N2 viruses have evolved specificity for extended, branched human-type receptors, conferring potential for increased avidity. *Cell Host Microbe* **21**, 23–34 (2017). doi:10.1016/j.chom.2016.11.004 Medline

83. R. Lei, W. Liang, W. O. Ouyang, A. Hernandez Garcia, C. Kikuchi, S. Wang, R. McBride, T. J. C. Tan, Y. Sun, C. Chen, C. S. Graham, L. A. Rodriguez, I. R. Shen, D. Choi, R. Bruzzone, J. C. Paulson, S. K. Nair, C. K. P. Mok, N. C. Wu, Epistasis mediates the evolution of the receptor binding mode in recent human H3N2 hemagglutinin. *Nat. Commun.* **15**, 5175 (2024). doi:10.1038/s41467-024-49487-4 Medline

84. V. B. Chen, W. B. Arendall 3rd, J. J. Headd, D. A. Keedy, R. M. Immormino, G. J. Kapral, L. W. Murray, J. S. Richardson, D. C. Richardson, MolProbity: All-atom structure validation for macromolecular crystallography. *Acta Crystallogr. D Biol. Crystallogr.* **66**, 12–21 (2010). doi:10.1107/S0907444909042073 Medline